20 Feb 2004

Analyzing and Modeling of Photobioreactors by Combining First Principles of Physiology and Hydrodynamics

Hu Ping Luo

Muthanna H. Al-Dahhan
Missouri University of Science and Technology, aldahhanm@mst.edu

Recommended Citation

H. P. Luo and M. H. Al-Dahhan, "Analyzing and Modeling of Photobioreactors by Combining First Principles of Physiology and Hydrodynamics," *Biotechnology and Bioengineering*, vol. 85, no. 4, pp. 382 - 393, Wiley, Feb 2004.
The definitive version is available at https://doi.org/10.1002/bit.10831

eppendorf

Boost Your (Stem) Cell Culture

We assist you to scale up your bioprocess –
Eppendorf Bioprocess Solutions for Cell & Gene Therapy Development - Flexibe, Scalable, Industrial

The BioFlo® 320 offers flexibility, better control, and maximum functionality while occupying a fraction of the valuable lab space of similar systems. This means greater efficiency and productivity at a lower operating cost for your lab. BioBLU® Single-Use Bioreactors were developed as true replacements for existing reusable vessels.

- > Sterility Assurance Level (SAL): 10^{-6}
- > Simplified handling reduces cross-contamination
- > Reliable scalability from 250 mL - 40 L through industrial design
- > Proven for animal and human cell lines
- > Increased productivity with reduced turnaround time between runs

www.eppendorf.com/BioBLUc

Analyzing and Modeling of Photobioreactors by Combining First Principles of Physiology and Hydrodynamics

Hu-Ping Luo, Muthanna H. Al-Dahhan

Bioprocess and Bioreactor Engineering Laboratory (BBEL), Chemical Reaction Engineering Laboratory (CREL), Department of Chemical Engineering, Washington University, One Brookings Drive, Campus Box 1198, St. Louis, Missouri 63130-4899; telephone: 314-935-7187; fax: 314-935-7211; e-mail: muthanna@che.wustl.edu

Received 26 March 2003; accepted 14 August 2003

Published online 13 January 2003 in Wiley InterScience (www.interscience.wiley.com). DOI: 10.1002/bit.10831

Abstract: Mixing in photobioreactors is known to enhance biomass productivity considerably, and flow dynamics play a significant role in the reactor's performance, as they determine the mixing and the cells' movement. In this work we focus on analyzing the effects of mixing and flow dynamics on the photobioreactor performance. Based on hydrodynamic findings from the CARPT(Computer Automated Radioactive Particle Tracking) technique, a possible mechanism for the interaction between the mixing and the physiology of photosynthesis is presented, and the effects of flow dynamics on light availability and light intensity fluctuation are discussed and quantitatively characterized. Furthermore, a dynamic modeling approach is developed for photobioreactor performance evaluation, which integrates first principles of photosynthesis, hydrodynamics, and irradiance distribution within the reactor. The results demonstrate the reliability and the possible applicability of this approach to commercially interesting microalgae/cyanobacteria culture systems. © 2004 Wiley Periodicals, Inc.
Keywords: photobioreactor; CARPT; hydrodynamics; airlift column; dynamic simulation

INTRODUCTION

The commercial potential of microalgae and cyanobacteria culturing has been well recognized for some time (Becker, 1994; Vonshak, 1992). However, there are few industrial efforts at the mass production of microalgae/cyanobacteria, especially for closed culturing of high value products, such as polyunsaturated fatty acids and red antiviral polysaccharides (RMP), etc. One of the major reasons for such slow industrial progress is the prohibitively high cost of production (Becker, 1994). This cost is a result of low area; or volume biomass productivity and the difficulties of design and scale-up of the photobioreactors (PBR).

Correspondence to: Muthanna H. Al-Dahhan

The growth of microorganisms in photobioreactors is a very complex system, coupling the effects of photosynthesis, reactor flow dynamics, and irradiance distribution within the photobioreactors (Luo et al., 2003). In fact, due to the severe self-shading effects of the cells in photobioreactors, especially with industrially interesting dense culturing and strong external irradiance, the light intensity decreases exponentially from the illuminated surface to the reactor center (i.e., following the Lambert-Beer law). Thus, a large dark zone in the center and a small highly illuminated zone near the surface coexist in a PBR. Both of the zones are not appropriate for cell's growth, since high light intensity may cause photoinhibition (Barber and Andersson, 1992), while low light intensity may not support the needed growth (photolimitation). Hence, the major factor controling the reactor performance is the availability and the intensity of light transferred to the cells (Merchuk et al., 1998).

Mixing, which governs the movements of the cells between the illuminated and the dark zones, can considerably enhance productivity for a wide range of operational conditions, as it can create beneficial light fluctuations onto the cells (Laws et al., 1983; Markl, 1980; Merchuk et al., 1998; Phillips and Myers, 1954; Terry, 1986; Winokur, 1948). However, the flow dynamics in photobioreactors and how flow dynamics interact with the photosynthesis processes remain unclear. As a consequence, most current studies analyze photobioreactor performance based on empirical correlations of the photosynthesis rate with limited reactor flow dynamic information, which can be applied only to specific conditions (Aiba, 1982; Jassby and Platt, 1976; Rorrer and Mullikin, 1999). The design and scale-up of PBRs based on these models require costly and labor-intensive empirical developmental efforts. Accordingly, a thorough analysis of the effects of flow dynamics on the photobioreactor performance, e.g., the interaction between mixing and photosynthesis, the effects of flow dynamics on the availability and the fluctuation of light experienced by

the cells, the effects of shear stress on the cells' growth, etc., is required for reactor design and scale-up. Moreover, a fundamentally based modeling approach that integrates first principles will facilitate reactor design and scale-up to maximize biomass productivity.

By employing an advanced flow dynamic measurement technique named CARPT (Computer Automated Radioactive Particle Tracking), Luo et al. (2003) investigated the flow dynamics in three types of airlift photobioreactors (bubble column, draft tube and split airlift columns), paying special attention to the local characteristics of the turbulent flow. They found that three types of liquid-phase mixing mechanisms coexist in the studied airlift columns. They are: bulk circulation with a time scale of 10 seconds, spiral movement with a time scale of seconds, and radial fluctuation due to turbulence with a time scale of milliseconds. Hence, the time scales associated with the induced light fluctuation experienced by the cells are not only in seconds, as reported by some researchers (Lee and Pirt, 1981), but also in milliseconds, which overlap with the range of time scales associated with the photosynthesis processes (Falkowski and Raven, 1997). Thus, a prompt relaxation of the reaction centers in the microorganisms from over-reduction is possible, which could improve the photosynthesis efficiency considerably. In fact, for a cell shifting between the highly illuminated and the dark zones, the overall photosynthetic quantum yield and the photosynthesis rate depend on the residence times in each zone. If the cell can be moved to the dark center from the highly illuminated zone before all reaction centers are reduced, it is possible to keep the quantum yield and, therefore, the light energy efficiency remains at a high level. Moreover, this shifting can also greatly reduce the photoinhibition effect, as the prompt ''relaxation'' prevents the proteins responsible for the photoinhibition effects from becoming overoxidized. This is very important for commercial culturing, where strong external irradiance is used. Based on such information, we can analyze the interaction between the mixing and the photosynthesis and characterize the light fluctuations experienced by the cells in the reactor.

Since mixing enhances reactor performance largely by introducing light fluctuations that change the pattern of light transferred to the cells, how photosynthetic rate responds to variant irradiance received by the cells is critical for the reactor performance evaluation (Crill, 1977; Eilers and Peeters, 1988, 1993; Pahl-Wostl and Imboden, 1990; Phillips and Myers, 1954). Two types of models exist in the literature to relate the photosynthesis rate with irradiance. The static models, based on fitting the photosynthesis-irradiance (P-I) curve, were developed empirically or semi-empirically for specific cases (e.g., optically dilute culture, low external light intensity) (Iwakuma and Yasuno, 1983; Jassby and Platt, 1976; Molina Grima et al., 1994). Due to their simplicity, most current studies for photobioreactor performance evaluation and reactor design are based on these static models. However, although these models fit reasonably with observations, they lack generality. They take into account only the amount of irradiance on a volume-averaged basis, ignoring the dynamic nature—the fact that light is fluctuating. And only a few of them consider the photoinhibition effects.

On the contrary, dynamic models (Camacho Rubio, et al., 2003; Eilers and Peeters, 1988, 1993; Han, 2001, 2002; Han et al., 2000; Magard et al., 1984; Pahl-Wostl and Imboden, 1990; Zonneveld, 1997, 1998) try to establish a physiological relationship between photosynthesis rates and irradiance. The advantage of these models is their ability to represent photoinhibition and other important physiology phenomena. However, the information of cells' movement, or the time series of light transferred to the cells, is required to implement such dynamic models to evaluate the reactor performance. Unfortunately, such Lagrangian information of cells' movement has not been available until recently (Luo et al., 2003) due to the need for advanced hydrodynamic measurement techniques. As a result, Wu and Merchuk (2002) used a trajectories predicted by a multi-circulation cells model (Joshi and Sharma, 1979) where such circulation cells are physically unrealistic (Degaleesan, 1997; Luo et al., 2003).

In this work, the effects of flow dynamics on the overall reactor performance are discussed and a fundamentally based modeling approach for reactor performance evaluation, based on the findings of hydrodynamics information obtained from the CARPT technique (Luo et al., 2003), is developed. The mixing-induced light intensity fluctuations delivered to the cells in the reactors are also quantitatively characterized. The developed modeling approach integrates a physiologically based dynamic photosynthetic model with CARPT measured hydrodynamics information. It is noteworthy that, although the photosynthetic model proposed by Eilers and Peeters (1988) and the Lambert-Beer law for the irradiance distribution inside the bioreactor were used in this work, the new approach can be extended to other

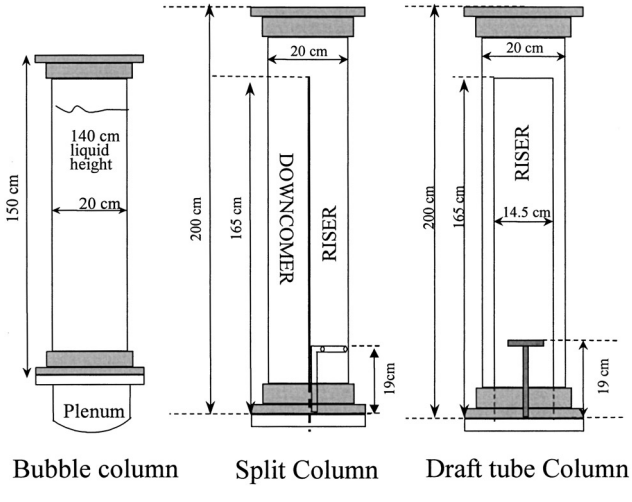

Figure 1. Configuration of the three types of photobioreactors studied in this work (Luo et al., 2003).

photosynthesis rate and irradiance distribution models based on first principles.

EXPERIMENTAL PROCEDURES

CARPT Experiments and Temporal Irradiance Pattern

In CARPT experiments, a small (2.3 mm), neutrally buoyant, and fully wet radioactive particle was used to follow the liquid phase flow and to mimic the cells' movement. The instantaneous particle position is identified by monitoring simultaneously the radiation intensities at a set of sodium iodide detectors (28) located strategically around the column. The details of these experiments and the measurement technique can be found elsewhere (Luo et al., 2003). Such CARPT experiments were implemented in three airlift bubble columns, shown in Figure 1, using an air–water system at two superficial gas velocities, 1 cm/s and 5 cm/s (Luo et al., 2003). All the reactors were Plexiglas columns of 8-inch diameter, either without internal structures (bubble column) or with different internal structures (split plate for split airlift column, and draft tube for draft tube airlift column). Different types of sparger were used to generate

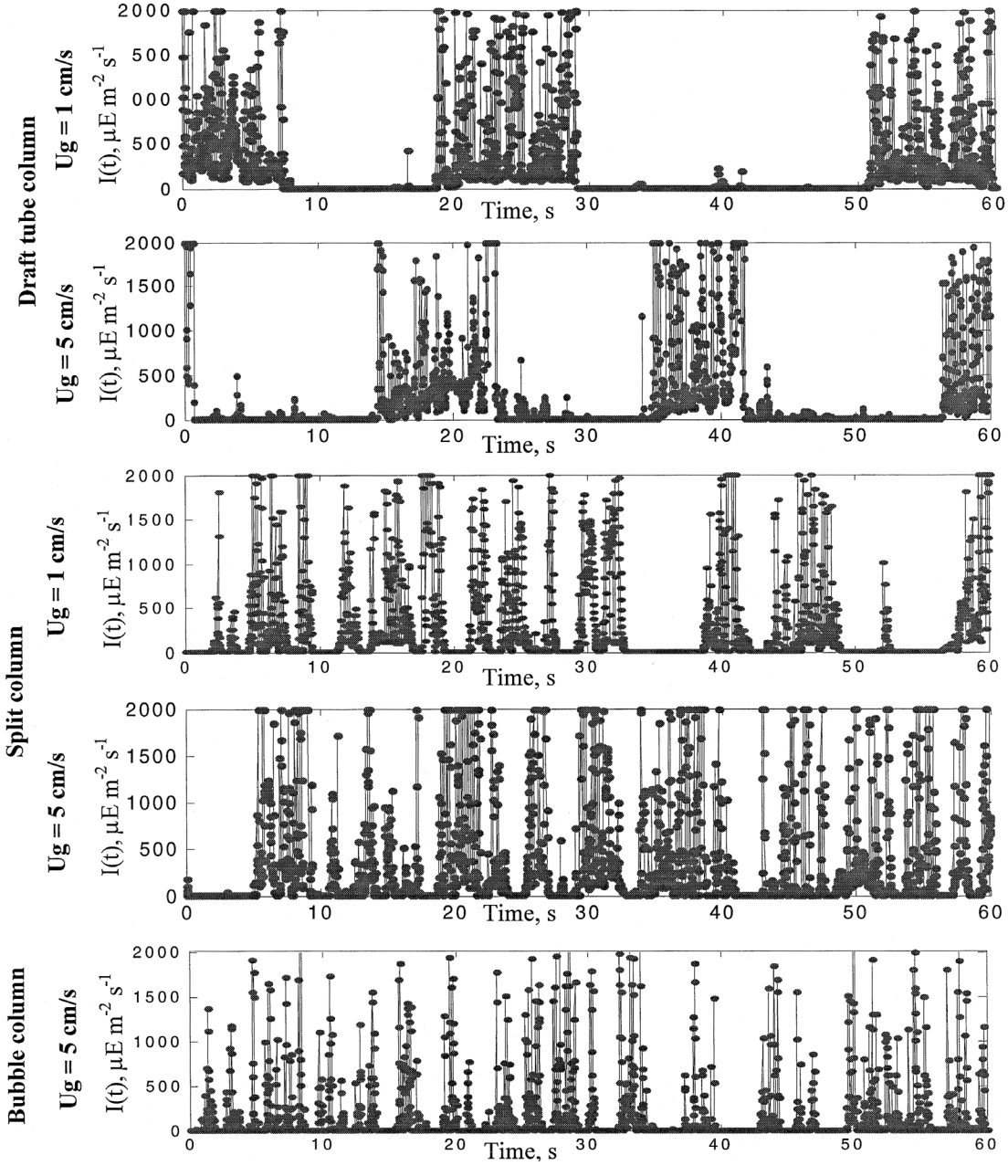

Figure 2. Time series of irradiance a cell experienced in the bioreactors. Calculated by Eq. (1). External irradiance: 2000 μE $m^{-2}s^{-1}$, Cell concentration: 80×10^6 cells/mL.

rather evenly distributed gas holdup. Each CARPT experiment was performed for 24 hours at a sampling frequency of 50 Hz, which generated Lagrangian trajectories of the tracer particle consisting of more than 4 million points (the time-averaged velocity at each point reach a plateau value which indicates statistically sufficient experimental time).

For each single cell in the photobioreactor, the time series of the irradiance it experiences, named the temporal irradiance pattern, can be calculated by combining CARPT measured cell's trajectories (Luo et al., 2003) with a proper irradiance distribution model. In this work, for simplicity and for demonstration purposes, the simple Lambert-Beer Law for a single light ray, which is suitable for a collimated irradiance model but is not for a diffuse or semi-diffuse model as explained by Evers (1991), is used for the light intensity distribution within the reactors:

$$I = I_E \cdot \exp[-(k_x \cdot x + k_w) \cdot d] \tag{1}$$

where I_E is the external irradiance on the photobioreactor surface; d is the radial distance from the cell to the illuminated surface; k_w and k_x are extinction coefficients accounting for water and the self-shade effects between cells, respectively; and x is the cells' concentration. The calculated temporal irradiance patterns for the studied airlift bubble columns have been shown in Figure 2. All of the characterizations and discussions presented later in this work are based on these calculated irradiance patterns.

MODELING APPROACH

Dynamic Modeling Approach For Reactor Performance Evaluation

A fundamentally based modeling approach would greatly benefit reactor design and scale-up to maximize biomass productivity. Such an approach should consider the physiology of photosynthesis and microorganism growth, the flow dynamics, and the irradiance distribution within the reactors. To begin, we need a dynamic photosynthesis rate model.

Many dynamic photosynthesis models use the concept of photosynthetic factory (PSF). Typically, it is assumed that the PSF has three states, or two states when the inhibition effect is ignored: reactive, activated, and inhibited (or inactivated). The interchange between these states represents different enzyme reactions, e.g., the light, the dark, and the inhibition reactions. The advantage of these models with three states is their ability to represent photoinhibition at supra-irradiance, and the differential equations thus generated are easily handled. However, due to the simplification of these models, normally not all physiology of the photosynthesis has been accounted for, e.g., the photoadaptation effect. Recently, Han (2001, 2002) reviewed such models and incorporated more physiology to generate a four-parameter model. While Camacho Rubio et al. (2003) proposed a mechanistic model by breaking down the photosynthesis process into two steps: a photochemical energy capturing step and a metabolic consumption step. This model takes into account the photoadaptive responses, photoinhibition, and the flashing light effect, which, inevitably, generated a few rather mathematically complex equations.

Unfortunately, although many models have been developed, further verification and model parameter estimation are very scarce in the literature. Merchuk et al. (1998, 2000) and Wu and Merchuk (2001, 2002) experimentally investigated the effects of well-defined light/dark cycles with different periods and light/dark ratios on the photosynthetic rate of a red marine microalgae, *Porphyridium* sp. Using the obtained experimental data, they estimated the model parameters of the dynamic model proposed by Eilers and Peeters (1988). And an additional maintenance term has been introduced to account for the cellular damage under detrimental culturing conditions, e.g., in cases of high shear stress and very low light intensity the photosynthesis rate can be negative. Hence, this model is used in this study and is further discussed in the following sections.

Three-State Photosynthesis Rate Model

The structure of the model developed by Eilers and Peeters (1988) and advanced by Wu and Merchuk (2001) is shown in Figure 3. This model assumes that PSF has three states: the resting state, x_1, the activated state, x_2, and the inhibited state, x_3. The probabilities of the state transitions following a photon capture are supposed to be proportional to the light intensity, or these reactions are assumed to be first-order reactions with reaction constants of αI for $x_1 \rightarrow x_2$ and βI for $x_2 \rightarrow x_3$. Since the other-state transitions can happen in the dark, the reaction constants for these reactions are assumed to be constant, i.e., δ for $x_2 \rightarrow x_1$, and γ for $x_3 \rightarrow x_2$. Thus, the following differential equations are proposed in the model:

$$\frac{dx_1}{dt} = -\alpha I \cdot x_1 + \gamma \cdot x_2 + \delta \cdot x_3 \tag{2}$$

$$\frac{dx_2}{dt} = \alpha I \cdot x_1 - \gamma \cdot x_2 - \beta I \cdot x_2 \tag{3}$$

$$\frac{dx_3}{dt} = \beta I \cdot x_2 - \delta \cdot x_3 \tag{4}$$

and

$$x_1 + x_2 + x_3 = 1 \tag{5}$$

where x_1, x_2, x_3 are the fractions of the PSFs in the resting, activated, and inhibited state, respectively. I is the instant light intensity experienced by the cells, $I(t)$, and α, β, δ, γ are the reaction constants.

The specific photosynthetic rate (μ) is proportional to the number of the state transitions from x_2 to x_1, the dark reaction:

$$\frac{1}{x}\frac{dx}{dt} = \mu = k \cdot \gamma \cdot x_2 - Me \tag{6}$$

where x is the total number of PSFs, and k is the yield of the photosynthesis reaction. *Me* is a maintenance constant accounting for cellular damage due to adverse environments, e.g., high shear stress. Wu and Merchuk (2002) defined *Me* as:

$$Me = \overline{Me} \cdot e^{k_m(\tau - \tau_c)} \tag{7}$$

where $\overline{Me}$ is the maintenance without shear stress effects, k_m is the extinction coefficient for shear stress, τ is shear stress, and τ_c is a constant that represents the critical level of shear stress below which no effect of shear stress on the growth is observed.

For the growth of *Porphyridium* sp., the parameters used in the equations are estimated by Wu and Merchuk (2002) and are shown in Table I.

Numerical Solution

Generally, the differential equations [Eqs. (2)–(5)] for the photosynthetic rate are a linear initial value problem for given values of the model parameters. For a given light intensity, i.e., I is constant, these equations can be solved explicitly by classical methods. Assuming the system reaches steady state, the analytical solution (Eilers and Peeters, 1988) of the system gives the photosynthetic rate for a given light intensity, which actually provides the photosynthesis-irradiance (*P-I*) curve shown in Figure 4 (for *Porphyridium* sp.), where x_1, x_2, x_3 profiles are shown as well. As can be seen, the specific growth rate reaches a maximum, or the saturation level, at 250 $\mu Em^{-2}s^{-1}$.

For cells growth in a real photobioreactor, numerical methods are required to solve the differential equations due to the chaotic nature of the temporal irradiance patterns (i.e., I varies with time). The cells' trajectories measured by CARPT experiments consist of successive sampling points

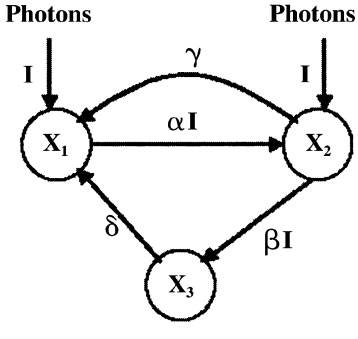

Figure 3. Structure of the photosynthetic rate model proposed by Eilers and Peeters (1988) (duplicated from Wu and Merchuk, 2001).

Table I. Parameters of the dynamic photosynthesis rate model for *Porphyridium,* sp. (Wu and Merchuk, 2002).

Parameter	Unit	Value
k	Dimensionless	3.65×10^{-4}
k_m	Pa^{-1}	1.6×10^{-3}
k_w	m^{-1}	0.2
k_x	ml $m^{-1}/10^6$ cell	3.0
$\overline{Me}$	s^{-1}	1.64×10^{-5}
α	$(\mu E\ m^{-2})^{-1}$	1.935×10^{-3}
β	$(\mu E\ m^{-2})^{-1}$	5.7848×10^{-7}
δ	s^{-1}	4.796×10^{-4}
γ	s^{-1}	0.1460
τ_c	Pa	2400

at frequency of 50 Hz. Between the short intervals of any two successive samples, the cells' concentration and the irradiance distribution inside the reactor can be assumed to be constant. Hence, the instant light intensity at any point between the two sampling points, *I(t)*, can be estimated by linear interpolation based on Eq. (1) (Evers, 1991) for simplicity and demonstration purpose:

$$I(t) = I_E \cdot exp\left\{-(k_x \cdot x^j + k_w) \cdot \left[d^j + \frac{t - t^j}{t^{j+1} - t^j}(d^{j+1} - d^j)\right]\right\}$$
$$t^j < t < t^{j+1}, j = 1, N-1 \tag{8}$$

where N is the total number of the trajectory points, and d is the distance to the illuminated surface. Therefore, the overall growth rate can be obtained by integrating the governing differential equations [Eqs. (2)–(5)] along the whole cell's trajectory from point to point.

The initial conditions we used in the simulation are:

$$x_1 = 1,\ x_2 = x_3 = 0, \qquad t = 0 \tag{9}$$

These conditions assume all cells are in the resting state as if they had been kept in dark for a long time. To account

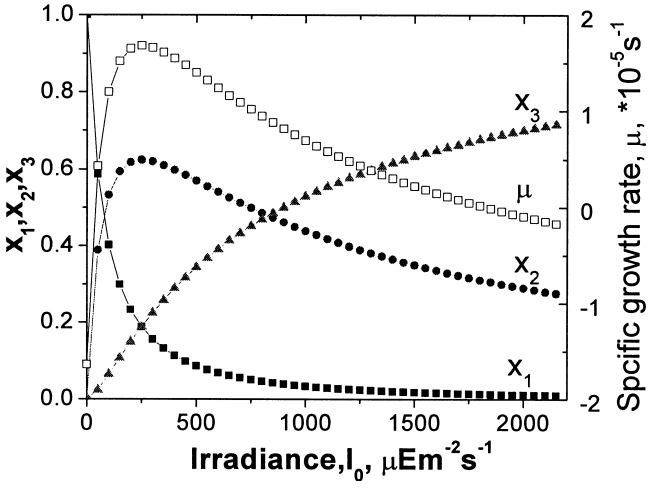

Figure 4. Computed photosynthesis-irradiance (P-I) curve together with profiles of PSF states by the dynamic photosynthesis rate model proposed by Eilers and Peeters (1988) for *Porphyridium,* sp. See text for details.

for the effects of shear stress, the time-averaged shear stress obtained from CARPT experiments was used to calculate the maintenance constant, *Me*, by Eq. (7).

Reactor Performance Simulation

The dynamic model has been implemented for the studied draft tube column at a superficial gas velocity of 1 cm/s. The simulation results were compared with the experimental data obtained by Merchuk et al. (2000), whose experiments were carried out in a different draft tube column, with a diameter of 0.13 m and a superficial gas velocity of 0.82 cm/s. Both the experimental data and the simulation results in this work are depicted in Figure 5, together with the simulation results of Wu and Merchuk (2002), which were obtained by integrating the governing equations along imaginary trajectories predicted by the circulation cell model (Joshi and Sharma, 1979). For comparison of the experimental data over 10 days, the numerical simulation was performed 10 times based on the same 24-h CARPT trajectory. This repetition is justified by the assumption of ergodicity of the tracking particle in CARPT experiments. As can be seen, without any fitting parameters, the simulation results of this work predict the experimental data reasonably well, with small discrepancies largely due to the different reactor and operation conditions used.

Additional Characterization of Photobioreactors in Terms of Light Fluctuation

To investigate the effects of light fluctuations on microorganism growth, many researchers have simply utilized a light on/off pattern, the so-called light/dark cycle as shown in Figure 6a. This pattern mimics the light fluctuation experienced by cells in photobioeactors as if the cells grow in a thin and sparse culturing system (Janssen et al., 2000, 2001; Nedbal et al., 1996; Terry, 1986; Wu and Merchuk, 2001). Terry (1986) proposed three parameters to characterize this well-defined light/dark cycle: incident light intensity (I_E), fluctuation frequency (f), and fraction of the light time in a cycle (also called dimensionless relaxation time, φ). The fluctuation frequency and the dimensionless relaxation time are defined as:

$$f = 1/(t_d + t_l); \qquad \varphi = t_l/(t_l + t_d) \tag{10}$$

where t_l is the time when the light is on, and t_d is the time when the light is off in one cycle. Using these parameters, the square wave signals or the light intensity fluctuations on the cells are clearly and completely defined. Terry (1986) proposed that the effects of the light fluctuations on the cell's growth are a function of these parameters. He assumed that, at high flash frequencies, the photosynthetic rate was determined by the average intensity received by the cells (full light intensity integration), while at low frequencies the cells responded to the instantaneous intensity (no light intensity integration).

However, as shown in Figure 2, it's hard to find the well-defined light/dark cycles in the chaotic temporal irradiance patterns. Therefore, to characterize the irradiance pattern in real reactors, the principles of how mixing affects the photosynthesis rate should be applied. As mentioned above, the quantum yield can be kept at a high level because of the relaxation of the cells shifting between the illuminated zone and the dark zone. In fact, since the time scales of the micro-eddy mixing and the photosynthesis electron transfer are both in milliseconds, a cell is likely to be ''over-charged'' whenever it enters the highly illuminated zone, where the light intensity is higher than the saturated light intensity. On the other hand, when a cell enters the dark zone, where its light intensity is lower than the saturated light intensity, the cell is likely to be ''relaxed.'' This could be further

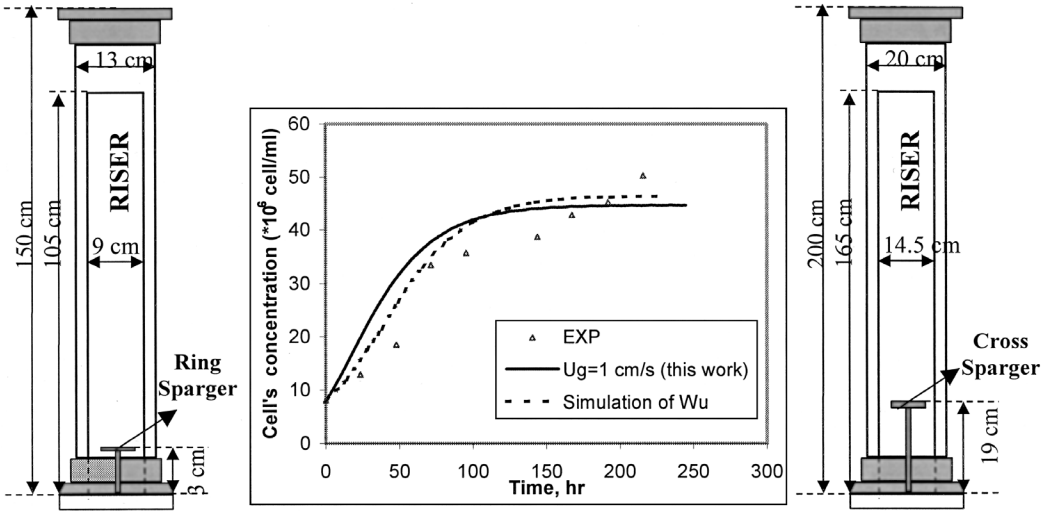

Figure 5. Simulation results by the dynamic model for the draft tube column (on the right) at Ug of 1 cm/s (based on the whole cross-section of the reactor). The experimental data (Merchuk et al., 2000) and simulation results of Wu (2001) are also presented, which are based on the draft tube column on the left at the superficial gas velocity of 0.82 cm/s.

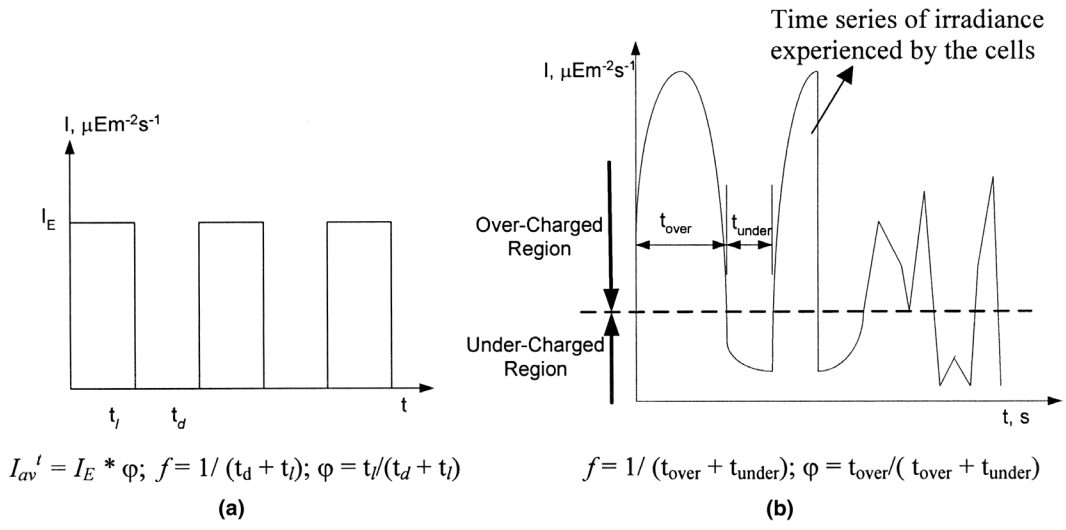

Figure 6. Illustration of the parameters to characterize the dynamic feature of irradiance fluctuation. (a) well-defined light/dark cycle; (b) over-/undercharged cycle in real reactors.

explained by the classical photosynthesis-irradiance (P-I) curve as shown in Figure 7. When the incident light intensity is very low as in the case of ''dark zone,'' the overall quantum yield is high and the photosynthesis rate increases linearly as the light intensity increases. This is called the undercharged region in the P-I curve. While when the incident light intensity exceeds the saturation light intensity as in the case of the ''highly illuminated zone'' in the reactor, the overall quantum yield could be very low and the photosynthesis rate reaches a plateau. This is called the over-charged region in the P-I curve. As the incident light increases further, some of the proteins in the electron transfer chain may be damaged and need a long time for recovery, resulting in a sudden drop of the photosynthesis rate. This is called the super-charged region in the P-I curve. Hence, separated by the saturation irradiance, the time series of irradiance could be roughly divided into two regions: overcharged and undercharged. The time series of the light intensity delivered to the cells can be decomposed into many such over-/undercharged cycles with different frequencies. These over-/undercharged cycles, following Terry's analysis for the well-defined light/dark cycle, can be characterized by three parameters: time-averaged light intensity (I_{av}^t) for the quantity of photons delivered to the cells, frequency (f) for the light fluctuation, and the fraction of over-charged time in a cycle (φ) for the dimensionless relaxation time. Figure 6b is a schematic diagram that illustrates these proposed parameters to characterize the dynamic feature of the light fluctuations.

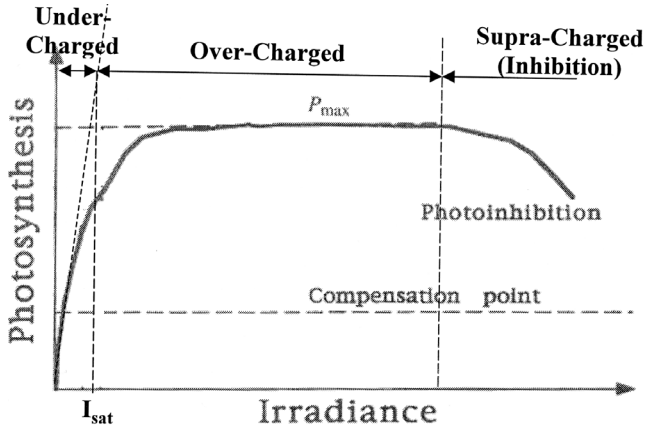

Figure 7. Typical photosynthesis-irradiance (P-I) curve (modified from Vonshak, 1992).

Once the over-/undercharged cycles are identified from the temporal irradiance patterns (typically around 4000 such over-/undercharged cycles per hour could be identified from the temporal irradiance patterns shown in Fig. 2), the dynamic nature of the light fluctuation can be characterized by statistical methods, e.g., by the probability density function (PDF) of these three parameters mentioned above. Accordingly, the effects of the reactor geometry and the operational parameters on the irradiance pattern, and hence, on the overall reactor performance, can possibly be further analyzed and used for reactor design and scale-up.

Average Irradiance

The amount of the irradiance a cell experiences can be represented by the time-averaged irradiance:

$$I_{av}^t = \frac{1}{T}\int_0^T I(t)dt \qquad (11)$$

where T is a very long time that covers all frequencies of irradiance fluctuation, and I(t) is the instant irradiance the cell experiences. It is noteworthy here that this definition is different from the one used by most authors in the

literature, which is actually a volume-averaged irradiance (Molina Grima et al., 1997):

$$I_{av}^{V} = \frac{1}{V}\int_{0}^{V} I_{Pi}dV \tag{12}$$

where V is the reactor volume and I_{Pi} is the local irradiance value at the finite control volume dV. The time-averaged irradiance is a complex function of external irradiance, reactor geometry, flow dynamics, cell concentration and morphology, and even the absorption characteristics of the cellular pigment. The volume-averaged irradiance is equivalent to the time-averaged value only when the cells are distributed homogenously throughout the reactor (Molina Grima et al., 1999).

To show the differences between these two definitions, both of them have been used to estimate irradiance for the studied reactors. Two cases have been considered. Case I represents low external irradiance (250 μE $m^{-2}s^{-1}$) plus low cell concentration (8×10^6 cells/mL) (the same as the experimental conditions used by Wu and Merchuk, 2001). Case II represents high external irradiance (2000 μE $m^{-2}s^{-1}$, typical sunlight intensity at noon in the summer) plus high cell concentration (80×10^6 cells/mL). The computed mean and variance of the averaged irradiances are shown in Table II. As can be seen, all calculated average light intensities are lower than the saturation light intensity, indicating the overall light limitation for these cultures. It is clear from the results that the reactor geometry and the superficial gas velocities do not affect the volume-averaged irradiance but do affect the time-averaged irradiance. Moreover, the differences between the computed quantities are much larger in Case II than in Case I. These differences indicate that volume-averaged irradiance does not account for the effects of flow dynamics, which have significant influence in the case of dense culturing and strong external irradiance. Therefore, volume-averaged irradiance cannot represent the actual amount of irradiance the cells experience in the photobioreactor under these conditions.

The effects of reactor geometry and superficial gas velocity on the time-averaged irradiance can be discerned from the results given in Table II. As can be seen, the calculated quantities for the split column are larger than the quantities for the other reactors. This difference is because of the spiral movement observed in the split column (Luo et al., 2003), in which the cells may have more chances to visit the highly illuminated surface than to visit the dark center. By the contrast in the draft tube and the bubble columns, the cells are more likely to visit the dark center, because liquid flows faster in the center region than in the near wall region. The draft tube column has a larger I_{av}^{t} than the bubble column, since the liquid phase is forced to travel near the wall region (the downcomer), while it is not in the bubble column. On the other hand, increasing the superficial gas velocity will increase the time-averaged irradiance, as can be seen from the results listed in Table II. In fact, as the superficial gas velocity increases, the turbulence intensity increases and the thickness of the boundary layer near the wall tends to decrease. The cells thus can enter the wall's vicinity. Moreover, in the split column, when the superficial gas velocity increases, the spiral movement of the flow is more apparent (Luo et al., 2003), resulting in a larger diameter of circulation that increases the probability of the cells to visit the wall region as well.

Irradiance Fluctuations

It is clear from Figure 2 that the temporal irradiance pattern consists of a cascade of light fluctuations with different frequencies. Thus, to better present the light fluctuations and the dynamic nature of the system, statistical methods need to be used. In this work, the probability density functions (PDF) of the over-/undercharged cycle frequency and of the dimensionless relaxation time have been estimated for the studied reactors under Case II. In Figure 8, the PDFs of the over-/undercharged cycle frequencies are shown by plotting the frequencies (f) vs. the number of occurrences per hour. In Figure 9, to better show the randomness of the system, the PDFs of the dimensionless relaxation time are presented by plotting $-1n(1/\varphi - 1)$ vs. the number of occurrences per hour. This plot actually shows the PDFs of the over-/undercharged time ratio (t_{over}/t_{under}) in a logarithmic axis coordinate.

Due to the limited sampling frequency used in CARPT experiments (50 Hz) of Luo et al. (2003), the highest frequency observed is 25 Hz, and only discrete series are obtained in the frequency field. As can be seen from Figure 8, the probability of the fluctuations increases almost linearly as its frequency increases. On the other hand, Figure 9 shows

Table II. Average irradiance and variance for the photobioreactors. Unit: E m^{-2} s^{-1}.

		Draft tube column		Split column		Bubble column
Mean and variance		1 cm/s	5 cm/s	1 cm/s	5 cm/s	5 cm/s
Case I[a]	I_{av}^{t}	135.0 ± 65.7	140.0 ± 63.7	141.5 ± 63.3	152.7 ± 62.2	123.3 ± 60.1
	I_{av}^{V}			131.3		
Case II[b]	I_{av}^{t}	90.2 ± 297.2	93.8 ± 306.2	126.9 ± 389.9	174.9 ± 444.5	46.3 ± 231.3
	I_{av}^{V}			164.3		

[a]Case I: External irradiance: 250 μE m^{-2} s^{-1}; Cell concentration: 8×10^6 cells/mL.
[b]Case II: External irradiance: 2000 μE m^{-2} s^{-1}; Cell concentration: 80×10^6 cells/mL.

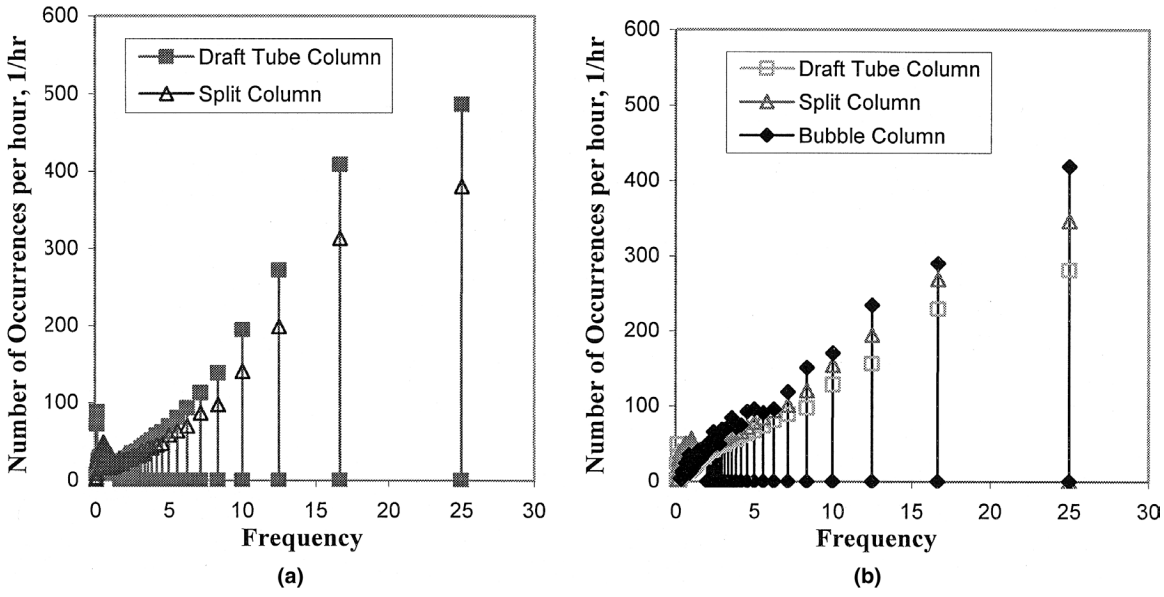

Figure 8. Probability density functions of the over-/undercharged cycle frequencies. External irradiance: 2000 μE $m^{-2}s^{-1}$, Cell concentration: 8 $\times 10^6$ cells/mL (a) Superficial gas velocity of 1 cm/s; (b) superficial gas velocity of 5 cm/s.

that the PDF of $-1n(1/\varphi - 1)$ is close to a Gaussian random distribution with a large peak in the center (i.e., overcharged time equals to undercharged time in a cycle). This Gaussian distribution indicates that the distribution of either the overcharged time or the undercharged time in a cycle is a random variable. In other words, around the saturation light intensity, I_{sat}, the cells have the same probability of entering the near wall region as of entering the center region. This is reasonable since the irradiance pattern is dominated by turbulence-induced fast fluctuations, and the turbulence is often considered as isotropic.

Again, the effects of reactor geometry and superficial gas velocity on the fluctuation can be found from these results (Figs. 8 and 9). The draft tube column possesses more fast light intensity fluctuations than the other reactors because the axial liquid flow in the near wall region, the downcomer in the draft tube column, is faster than the axial velocity in the other reactors at the same superficial gas velocity, suggesting larger turbulence intensity. In the split column, although the turbulence intensity in the wall region is large in the riser, it is not in the downcomer, which offsets its overall effects on the light intensity fluctuations. Very interestingly,

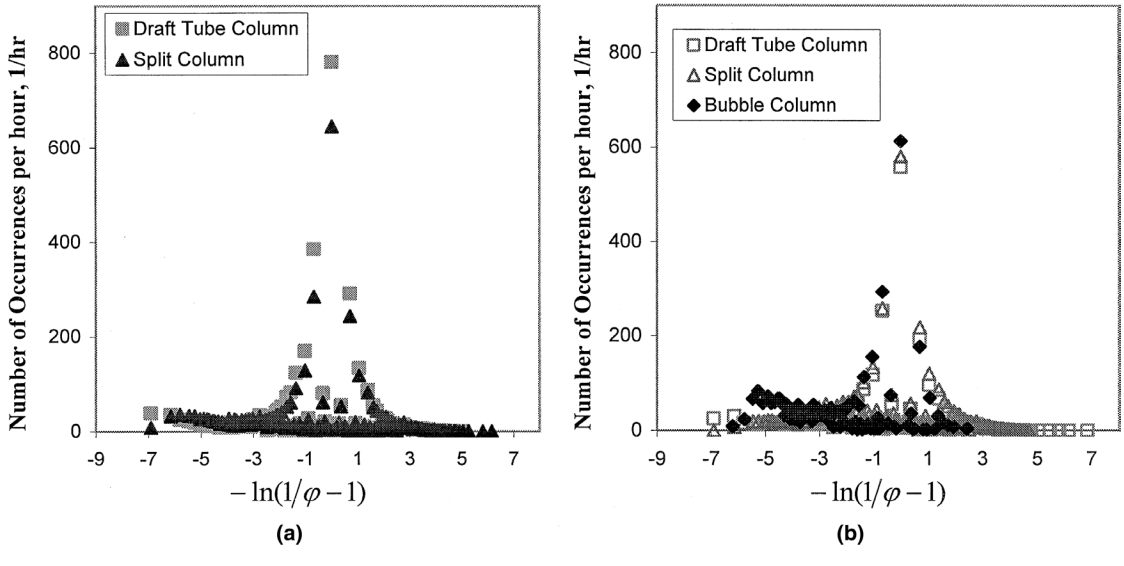

Figure 9. PDF of the dimensionless relaxation time presented by plotting $-1n(1/\varphi - 1)$ vs. the number of occurrence per hour, which in fact shows the PDF of the over-/undercharged time ratio (t_{over}/t_{under}) in a logarithmic axis coordinate. External irradiance: 2000 μE $m^{-2}s^{-1}$, Cell concentration: 8 $\times$ 10^6 cells/mL (a) Superficial gas velocity of 1 cm/s; (b) superficial gas velocity of 5 cm/s.

the superficial gas velocity shows a negative effect on the light intensity fluctuations: when it increases, the probabilities of the fast fluctuations decrease for both split and draft tube columns. This negative effect is inconsistent with the common-sense notion that more turbulence intensity means more light intensity fluctuations. The inconsistency suggests that the sampling frequency (50 Hz) used in these CARPT experiments may miss some higher frequency fluctuations. Actually, the liquid flow enters the so-called transitional regime at superficial gas velocity of 5 cm/s, and the time scales associated with the micro-eddies in such a regime can be in hundreds of microseconds. This difficulty would be greatly alleviated by increasing the sampling frequency, which currently can be as high as 500 Hz.

Effects of Reactor Geometry and Superficial Gas Velocity

Based on the dynamic model developed above, the overall growth rate of the cells in the three types of bioreactors are calculated and compared as shown in Figure 10. Obviously, the overall performance of the split column excels that of the draft tube and the bubble columns, and the superficial gas velocities positively affect the performance. These results are consistent with the above analysis concerning the effects of the reactor geometry and the operational conditions on the parameters characterizing the temporal irradiance pattern. For example, since the overall control factor for the photobioreactor performance is the light limitation (e.g., the time-averaged irradiances for all cases in Table II are smaller than the saturation light intensity), the overall performance for the reactors is strongly affected by the average irradiance. Hence, as the cells in the split column are able to receive more light than the cells in the other types of reactors (due to the spiral liquid phase flow), the overall growth rate is higher in this type of reactor. The results also reveal the effects of the light intensity fluctuations. For example, although I_{av}^{t} for the split column at an Ug of 1 cm/s is much larger than I_{av}^{t} for the draft tube column at the same superficial gas velocity, the overall performance for the split column is just slightly larger than that of the draft tube column. The irradiance patterns for the draft tube column consist of more fast fluctuations than the split column, indicating a better quantum yield. On the other hand, because of the chaotic nature of the fluctuations, the effect of the relaxation time is not clear in these cases. Actually, as can be seen from Figure 9, the profiles of the PDF for the relaxation time in all the cases almost collapse into one.

Accordingly, these proposed parameters, i.e., time-averaged irradiance (I_{av}^{t}), over-/undercharged cycle frequencies (f), and the dimensionless relaxation time (φ), can be used to characterize the availability and the fluctuation of light transferred to the cells—the controling factor of the photobioreactor performance. They integrate information of flow dynamics and irradiance transportation and are functions of reactor geometry, operational conditions, and the optical properties of the culturing media. With the future availability of experimental data bank and validated Computational Fluid Dynamics (CFD) codes, it is possible to estimate these proposed parameters for different reactor geometry and operating variables, which will provide a means to screen different reactor design and operating parameters for a desired photobioreactor's performance. In fact, these proposed parameters would also be correlated to the reactor performance based on Terry's (1986) assumption as mentioned above, which is beyond the scope of this work.

REMARKS

In this work, efforts have been focused on an analysis of the effects of mixing, or flow dynamics, on photobioreactor performance. Based on the hydrodynamic findings obtained by the CARPT technique (Luo et al., 2003), the effects of flow dynamics on light availability and light intensity fluctuations have been analyzed and quantitatively charac-

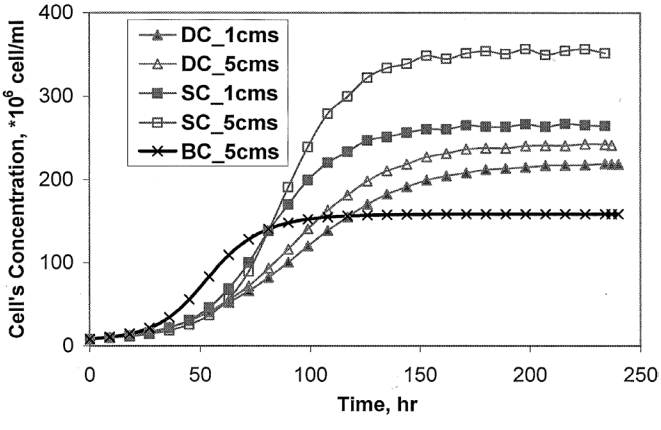

Figure 10. Numerical simulated cell's concentration profiles for different type of reactors and superficial gas velocities. Simulation condition: External irradiance: 2000 μE $m^{-2}s^{-1}$; Initial cells concentration: 8×10^6 cells/mL (BC: Bubble column; SC: Split column; DC: draft tube column.).

terized. Furthermore, a dynamic modeling approach has also been developed for photobioreactor performance evaluation. This general modeling approach integrates first principles of photosynthesis, hydrodynamics, and irradiance distribution within the reactor. It can be extended to include other physiologically based photosynthesis rate and irradiance distribution models, which may greatly improve the accuracy of and the reliability on the prediction of the cells growth and photobioreactor performance. However, the developed modeling approach requires Lagrangian trajectory information of the cells' movement in the reactors by CARPT. It is noteworthy that in case the CARPT technique is unavailable, particularly for large scale units, the needed information mentioned above can be obtained by implementing CFD codes provided that these codes are validated first, which is in progress in our laboratory. Hence, the developed modeling approach provides a direct and comprehensive tool for photobioreactor analysis, which should be essential for proper and efficient reactor design and scale-up for large-scale biomass production.

NOMENCLATURE

d	radial distance from the cells to the illuminated surface [m]
f	frequency of the light intensity fluctuations [s^{-1}]
I	instantaneous incident light intensity on the cells [$\mu Em^{-2}\ s^{-1}$]
I_E	external irradiance exposed to the photobioreactor surface [$\mu Em^{-2}\ s^{-1}$]
I_{av}^{t}	time-averaged light intensity [$\mu Em^{-2}\ s^{-1}$]
I_{av}^{V}	volume-averaged light intensity [$\mu Em^{-2}\ s^{-1}$]
I_{Pi}	local irradiance value at the finite control volume dV [$\mu Em^{-2}\ s^{-1}$]
I_{sat}	saturation light intensity [$\mu Em^{-2}\ s^{-1}$]
j	index of the sampling points
k	yield of photosynthesis production to the transition of x_2 to x_1[dimensionless]
k_m	extinction coefficient of shear stress in Eq. (7), [Pa^{-1}]
k_w	extinction constant for water in Eq. (1), [m^{-1}]
k_x	extinction constant for biomass in Eq. (1), [mL/(m · 10^6 cells)]
Me	maintenance in Eq. (7), [s^{-1}]
$\overline{Me}$	maintenance without shear stress effects in Eq. (7), [s^{-1}]
N	total number of sampling points
t_d	time when light is on in a light/dark cycle [s]
t_l	time when light is off in a light/dark cycle [s]
t_{over}	overcharged time in an over-/undercharged cycle [s]
t_{under}	undercharged time in an over-/undercharged cycle [s]
T	total sampling time [s]
Ug	superficial gas velocity [cm/s]
V	total volume of the bioreactor [m^3]
x	biomass concentration [10^6 cells/mL]
x_1	fraction of PSF in open state
x_2	fraction of PSF in closed state
x_3	fraction of PSF in inhibited state

Greek letters

μ	specific growth rate [s^{-1}]
τ	shear stress [Pa]
τ_c	critical shear stress in Eq. (7), [Pa]
α	rate constant of photon utilization to transfer x_1 to x_2 [$(\mu Em^{-2})^{-1}$]
γ	rate constant of transfer x_2 to x_1 [$(\mu Em^{-2})^{-1}$]
δ	rate constant of transfer x_3 to x_1 [$(\mu Em^{-2})^{-1}$]
β	rate constant of photon utilization to transfer x_2 to x_3 [$(\mu Em^{-2})^{-1}$]
φ	dimensionless relaxation time

The authors gratefully appreciate Dr. Fernandez Sevilla and Dr. Xiaoxi Wu for their valuable suggestions and comments on this work. We also thank the anonymous reviewers for stimulating comments on the manuscript.

References

Aiba S. 1982. Growth kinetics of photosynthetic microorganisms. Adv Biochem Eng 23:85–156.

Barber J, Andersson B. 1992. Too much of a good thing: Light can be bad for photosynthesis. Trends Biochem Sci 17:61–66.

Becker EW. 1994. Microalgae: Biotechnology and microbiology. In: J. Baddiley NH, Carey IJ, Higgins, Potter WG, editors. Cambridge studies in biotechnology, series 10. Cambridge, UK: Cambridge University Press.

Camacho Rubio F, Garcia Camacho F, Fernandez Sevilla JM, Chisti Y, Molina Grima E. 2003. A mechanistic model of photosynthesis in microalgae. Biotechnol Bioeng 81(4):459–473.

Crill PA. 1977. The photosynthesis-light curve: a simple analog model. J Theor Biol 64:503–516.

Degaleesan S. 1997. Fluid dynamic measurements and modeling of liquid mixing in bubble columns. Doctoral thesis, Washington University in Saint Louis, MO.

Eilers PHC, Peeters JCH. 1988. A model for the relationship between light intensity and the rate of photosynthesis in phytoplankton. Ecological Modeling 42:199–215.

Eilers PHC, Peeters JCH. 1993. Dynamic behavior of a model for photosynthesis and photoinhibition. Ecological Modeling 69:113–133.

Evers EG. 1991. A model for light limited continuous cultures. Biotechnol Bioeng 38:254–259.

Falkowski PG, Raven JA. 1997. Aquatic photosynthesis. London, UK: Blackwell Science.

Han B-P. 2001. Photosynthesis-irradiance response at physiological level: a mechanistic model. J Theor Biol 213:121–127.

Han B-P. 2002. A mechanistic model of algal photoinhibitoin induced by photodamage to photosystem-II. J Theor Biol 214:519–527.

Han B-P, Virtanen M, Koponen J, Straskraba M. 2000. Effect of photoinhibition on algal photosynthesis: a dynamic model. J Plankton Res 22:865–885.

Iwakuma T, Yasuno M. 1983. A comparison of several mathematical equations describing photosynthesis-light curve for natural phytoplankton populations. Arch Hydrobiol 97:208–226.

Janssen M, Janssen M, Winter M, Tramper J, Mur LR, Snel J, Wijffels RH. 2000. Efficiency of light utilization of *Chlamydomonas reinhardtii* under medium-duration light/dark cycles. J Biotechnol 78: 123–137.

Janssen M, Slenders P, Tramper J, Mur LR, Wijffels RH. 2001. Photosynthetic efficiency of Dunaliella tertiolecta under short light/dark cycles. Enzyme Microb Technol 29:298–305.

Jassby AD, Platt T. 1976. Mathematical formulation of the relationship between photosynthesis and light for phytoplankton. Limnol Oceanog 21:540–547.

Joshi JB, Sharma MM. 1979. A circulation cell model for bubble columns. Trans Ins Che Eng 57:244–251.

Laws EA, Terry KL, Wichman J, Chalup MS. 1983. A simple algal production system designed to utilize the flashing light effect. Biotechnol Bioeng 25:2319–2335.

Lee Y, Pirt SJ. 1981. Energetics and photosynthetic algal growth. Influence of intermittent illumination in short (40s) cycles. J Gen Microbiol 124:43–52.

Luo H-P, Kemoun A, Al-Dahhan MH, Fernández Sevilla JM, García Sánchez JL, García Camacho F, Molina Grima E. 2003. Analysis of photobioreactors for culturing high value microalgae and cyanobacteria via an advanced diagnostic technique: CARPT. Chem Eng Sci 58(12):2519–2527.

Magard RO, Tonkyn DW, Sehft WH. 1984. Kinetics of oxygenic photosynthesis in planktonic algae. J Plankton Res 6(2):325–337.

Markl H. 1980. Modeling of algal production systems. Amsterdam: Elsevier. p 361–383.

Merchuk JC, Gluz M, Mukmenev I. 2000. Comparison of photobioreactors for cultivation of the microalga *Porphyridium sp*. J Chem Technol Biotechnol 75(12):1119–1126.

Merchuk JC, Ronen M, Giris S, Arad S. 1998. Light/dark cycles in the growth of the red microalga Porphyridium Sp. Biotechnol Bioeng 59 (6):705–713.

Molina Grima E, Garcia Camacho F, Sanchez Perez JA, Fernandez Sevilla J, Acien Fernandez FG, Contreras Gomez A. 1994. A mathematical model of microalgal growth in light limited chmostat cultures. J Chem Technol Biotechnol 61:167–173.

Molina Grima E, Camacho FG, Peres JAS, Fernandez FGA, Sevilla JMF. 1997. Evaluation of photosynthetic efficiency in microalgal cultures using averaged irradiance. Enzyme Microb Technol 21:375–381.

Molina Grima E, Fernandez FGA, Camacho FG, Chisti Y. 1999. Photobioreactors: Light regime, mass transfer, and scaleup. J Biotechnol 70: 231–247.

Nedbal L, Tichy V, Xiong F, Grobbelaar JU. 1996. Microscopic green algae and cyanobacteria in high-frequency intermittent light. J Appl Phycol 8:325–333.

Palhl-Wostl C, Imboden DM. 1990. DYPHORA—A dynamic model for the rate of photosynthesis of algae. J Plankton Res 12(6):1207–1221.

Phillips JN, Myers J. 1954. Growth rate of *Chlorella* in flashing light. Plant Physiol 29:152.

Rorrer GL, Mullikin RK. 1999. Modeling and simulation of a tubular recycle photobioreactor for macroalgal cell suspension cultures. Chem Eng Sci 54(15–16):3153–3162.

Terry KL. 1986. Photosynthesis in modulated light: quantitative dependence of photosynthetic enhancement on flashing rate. Biotechnol Bioeng 28:988–995.

Vonshak A. 1992. Microalgal biotechnology: Is it an economic success? In: Da SilVa EJ, Ratledge C, Sasson A, editors. Biotechnology: Economic and social aspects, issue for developing countries. Cambridge, UK: Cambridge University Press.

Winokur M. 1948. Growth relationship of *Chlorella* species. Am J Bot 35:118–129.

Wu X, Merchuk JC. 2001. A model integrating fluid dynamics in photosynthesis and photoinhibition processes. Chem Eng Sci 56: 3527–3538.

Wu X, Merchuk JC. 2002. Simulation of algae growth in a bench-scale bubble column reactor. Biotechnol Bioeng 80(2):156–168.

Zonneveld C. 1997. Modeling effects of photoadaptation on the photosynthesis-irradiance curve. J Theor Biol 186:381–388.

Zonneveld C. 1998. Photoinhibition as affected by photoacclimation in phytoplankton: A model approach. J Theor Biol 193:115–123.